drones

MDPI

*Article*

# Safety-Critical Fixed-Time Formation Control of Quadrotor UAVs with Disturbance Based on Robust Control Barrier Functions

**Zilong Song [2] and Haocai Huang [1,2,3,4,*]**

[1] Donghai Laboratory, Zhoushan 316021, China
[2] Ocean College, Zhejiang University, Hangzhou 310058, China; zilong_song@zju.edu.cn
[3] Laboratory for Marine Geology, Qingdao Marine Science and Technology Center, Qingdao 266061, China
[4] Hainan Institute of Zhejiang University, Sanya 572025, China
* Correspondence: hchuang@zju.edu.cn

**Abstract:** This paper focuses on the safety-critical fixed-time formation control of quadrotor UAVs with disturbance and obstacle collision risk. The control scheme is organized in a distributed manner, with the leader's position and velocity being estimated simultaneously by a fixed-time distributed observer. Meanwhile, a disturbance observer that combines fixed-time control theory and sliding mode control is designed to estimate the external disturbance. Based on these techniques, we design a nominal control law to drive UAVs to track the desired formation in a fixed time. Regarding obstacle avoidance, we first construct safety constraints using control barrier functions (CBFs). Then, obstacle avoidance can be achieved by solving an optimization problem with these safety constraints, thus minimally affecting tracking performance. The main contributions of this process are twofold. First, an exponential CBF is provided to deal with the UAV model with a high relative degree. Moreover, a robust exponential CBF is designed for UAVs with disturbance, which provides robust safety constraints to ensure obstacle avoidance despite disturbance. Finally, simulation results show the validity of the proposed method.

**Keywords:** formation control; fixed-time control; control barrier functions; safety-critical control; obstacle avoidance; quadrotor UAVs



**Citation:** Song, Z.; Huang, H. Safety-Critical Fixed-Time Formation Control of Quadrotor UAVs with Disturbance Based on Robust Control Barrier Functions. *Drones* **2024**, *8*, 618. https://doi.org/10.3390/drones8110618

Academic Editors: Rodney Swee Huat Teo and Sunan Huang

Received: 1 August 2024
Revised: 10 October 2024
Accepted: 17 October 2024
Published: 28 October 2024



## 1. Introduction

Recently, the tracking control of UAVs has received widespread attention due to its tremendous applications [1], such as in transportation, environmental monitoring, and equipment maintenance. At the same time, we note that some work is difficult for individual UAVs to perform, and the collaborative cooperation of multiple UAVs is necessary [2,3]. In this way, the formation control of multiple UAVs becomes a worthwhile research topic [4]. Meanwhile, in special work scenarios, avoiding obstacles and ensuring the safety of UAVs is a topic of concern [5].

Much effort has been put into the formation tracking control of UAVs in recent years, and the control strategy has developed from centralized to distributed [6]. Compared to a centralized one, a distributed strategy allows each UAV to make decisions independently, and this parallelism improves computational efficiency and fault tolerance [7]. However, this inevitably makes formation control more difficult since the control laws deployed in followers cannot directly access the leader's state. Distributed observers [8–10] are commonly used to solve this problem, estimating the leader's state via information communication. Meanwhile, many concerns such as communication delays [11], packet discreteness [12], and link fault [13] have been focused on. Moreover, the convergence speed of the distributed observers needs to be considered; the asymptotical stable observers in [8,9] usually require more time to estimate the leader's state, and it would be great if we could perform this in a fixed/finite time. In this regard, finite-time distributed observers are proposed in [14,15] to estimate the leader's position, and fixed- and finite-time observers are used

in [16,17] to obtain the leader's velocity. However, few studies have been able to obtain the leader's position and velocity simultaneously in a fixed time.

Moreover, improving the performance of the control law is a continually popular topic of research, and the convergence time is a major concern. Much effort has been made to achieve the tracking of desired formations by UAVs in a finite/fixed time, and prescribed performance control (PPC) with a finite-time performance function is a commonly used technique [18–21]. However, the performance function imposes conditions on the initial state/error of the UAVs; also, with the limitation by the performance function, the tracking error cannot grow after convergence, which conflicts with the need for obstacle avoidance. Facing these problems, fixed-time control theory provides an approach in which the convergence time can be preset depending only on control parameters, and the constraint on the initial state/error is removed [22]. With these advantages, the fixed-time control strategy is widely used in UAV formation control [23,24]. Also, it combines with other advanced control technologies in its use in UAV formation control, such as fuzzy control [25], sliding mode control [26], and event-triggered control [27,28].

Furthermore, disturbance caused by air currents is unavoidable and therefore needs to be considered. Many powerful tools are proposed to address this problem, such as an extended state observer (ESO) [29], disturbance observer (DO) [30], neural network (NN) [31], adaptive fuzzy observer [32], and disturbance compensation [33]. Nevertheless, these techniques only achieve asymptotic or exponential stabilization, and a long convergence time is needed. The finite/fixed-time control method is combined with observers in the most recent studies. A finite-time ESO, which estimates the disturbance and unmeasured velocity in a finite time, is used in UAV formation control [10,34,35]; nevertheless, its convergence time strongly relies on the initial states. Also, fixed-time DOs are proposed in [36–38], with the shortcoming of needing the upper bound of the disturbance. Therefore, we can see that the designing of observers that can estimate disturbance in a fixed time and eliminate the need for prior knowledge of disturbance is an interesting topic.

It is important to note that many stationary or moving obstacles exist in the environment; thus, it is important to ensure that all UAVs can avoid collisions with these obstacles. Artificial potential functions (APFs) are commonly used for this purpose [39–41], which are directly added to the control law and provide repulsive force when facing obstacles. However, this is a straightforward method that modifies the control law, and the APF terms are commonly designed to be overly conservative. Thus, it may lead to over-conservative behaviors [42], and tracking performance will be greatly affected when facing obstacles, especially moving obstacles. Moreover, we note that UAVs are usually limited in the maximum speed and acceleration they can reach, and these limitations are termed state constraints. These state constraints are commonly ignored in APF-based obstacle avoidance control; thus, the APFs have the potential to be ineffective, especially in complex environments and when facing multiple obstacles. In recent works, safety-critical control, which places the highest priority on safety, has received widespread attention [43]. A novel control barrier function (CBF) is widely used in safety-critical control, which can provide safety constraints that ensure no collisions occur [44]. Then, obstacle avoidance can be achieved by solving the optimization problems with constraints constructed by CBFs. The advantages of optimized control enable tracking performance to be affected as little as possible during obstacle avoidance, and the state constraints can be considered at the same time in optimized control. Due to these advantages, CBF-based safety-critical control is used for obstacle avoidance in UAVs in the latest studies [42,45–47].

Despite these advantages, some challenges prevent their further application. The first one is that CBFs can only deal with systems with a relative degree of one, which means that the control inputs should appear in their first-order derivative [44,48]. Specifically, the dynamic model can only be a first-order system if we construct the position-based safety constraints, which prevents the application of CBFs in UAV systems since UAVs are commonly modeled by high-order systems [49]. Existing studies about the safety-critical control of UAVs actually employ the reduce-order strategy or the high-relative-degree CBF

constructing method to address this problem. Specifically, refs. [42,45] first obtain a safe velocity law via CBF-based optimization and then design a control law to track this safe velocity. However, since it takes time to track the desired safe velocity, this method may not work in a sudden crisis. Refs. [46,47] proposed a constructed high-relative-degree CBF for a UAV model; however, chattering during obstacle avoidance cannot be avoided due to the introduction of the derivative term in the CBF. Meanwhile, another concern is that an accurate model is needed when executing safety-critical control. We may obtain the wrong safety constraints constructed by CBFs when there are disturbances in the dynamic model. Then, wrong control input will be calculated via optimization with wrong safety constraints, and this leads to collisions. Some efforts have been made to address this problem. The Gaussian process (GP) is used in [50] to predict the uncertainty arising in CBFs at the cost of greatly increasing the computational burden [51], since the GP is a data-driven approach and has the complexity of $O(n^3)$ [52]. An input-to-state safety CBF is proposed in [53,54] to address input disturbances, and a robust safety-critical control method is used in [55] for sector-bounded disturbances. However, these methods can only deal with input-related disturbances. Thus, it makes sense to design a robust safety-critical control approach that can provide robust safety constraints for high-relative-degree UAVs with external disturbances.

Motivated by the above results, we design a safety-critical fixed-time control method for UAV formation with obstacle collision risk. The distributed nominal control law is fully designed in a fixed-time convergence form despite external disturbance. Moreover, obstacle avoidance is achieved via optimized control with the constraints being constructed using elaborate exponential robust CBFs. The main contributions of this work are listed as follows.

A fixed-time distributed observer is designed to estimate the leader's states in a fixed time; compared with the existing results [8,9,14–17], it can estimate the position and velocity simultaneously. Also, a disturbance observer combining fixed-time control strategy and sliding mode control strategy is designed to estimate the external disturbances; compared with the fixed-time disturbance observer in [23,56–58], it improves the performance and robustness of the system, owing to the use of sliding mode control.

We propose a CBF-based safety-critical control method to achieve obstacle avoidance, which can optimize nominal control law via a quadratic program with constraints established using control barrier functions. Compared with the control methods in [39–41] that add APFs directly to the control law, the outstanding feature of this method is that the nominal control law is only modified when collision is truly imminent, which guarantees that tracking performance is minimally affected.

An exponential CBF is proposed to establish two relative degree safety constraints for UAVs; compared with the existing reduce-order method [42,45,59] and the high-relative-degree CBF constructing method [46,47], this exponential CBF can ensure the performance and feasibility of the system. Meanwhile, CBFs are based on an accurate model, and external disturbance may lead to a violation of safety constraints; we combine the exponential CBF and min–max inequality to propose robust safety constraints, which can ensure UAV safety despite external disturbance.

The remainder of this paper is organized as follows. Section 2 presents the preliminaries. The designed nominal fixed-time control law is described in Section 3. The safety-critical formation control law is provided in Section 4. Simulation results are provided in Section 5.

## 2. Materials and Methods

### 2.1. Dynamic Model

We consider a group of quadrotor UAVs with one virtual leader and $N$ followers. According to [49], the dynamic model of a quadrotor UAV can be decomposed into the

outer loop (position) and the inner loop (attitude). The outer loop of quadrotor UAVs (position dynamic) with disturbances is given as

$$\begin{aligned}\ddot{x}_i &= -\tfrac{K_1}{m_i}\dot{x}_i + \tfrac{T_i}{m_i}(C(\varphi_i)S(\theta_i)C(\psi_i) + S(\varphi_i)S(\psi_i)) + d_{i,1}\\ \ddot{y}_i &= -\tfrac{K_2}{m_i}\dot{y}_i + \tfrac{T_i}{m_i}(C(\varphi_i)S(\theta_i)S(\psi_i) - S(\varphi_i)C(\psi_i)) + d_{i,2}\\ \ddot{z}_i &= -\tfrac{K_3}{m_i}\dot{z}_i + \tfrac{T_i}{m_i}(C(\varphi_i)C(\theta_i)) - g + d_{i,3}\end{aligned} \tag{1}$$

where $i \in \{1, \ldots, N\}$ denotes the $i$-th follower and $i = 0$ is the virtual leader. $C(\bullet) = \cos(\bullet)$, and $S(\bullet) = \sin(\bullet)$. $x_i$, $y_i$, and $z_i$ are the positions in the earth's inertial coordinate frame, and $\varphi_i$, $\theta_i$, and $\psi_i$ denote the roll, pitch, and yaw angle, indicating the UAV's attitude with respect to the inertial coordinate frame. $K_1$, $K_2$, and $K_3$ are the aerodynamic damping coefficient, $d_{i,j}$ are the bounded disturbances, $m_i$ is the mass of the $i$-th UAV, and $T_i$ is the thrust.

We define the position control input as

$$\begin{aligned}u_{i,x} &= \tfrac{T_i}{m_i}(C(\varphi_i)S(\theta_i)C(\psi_i) + S(\varphi_i)S(\psi_i))\\ u_{i,y} &= \tfrac{T_i}{m_i}(C(\varphi_i)S(\theta_i)S(\psi_i) - S(\varphi_i)C(\psi_i))\\ u_{i,z} &= \tfrac{T_i}{m_i}(C(\varphi_i)C(\theta_i))\end{aligned} \tag{2}$$

Then, the dynamics (1) can be rewritten as

$$\begin{aligned}\dot{p}_i &= v_i\\ \dot{v}_i &= \Gamma_i v_i + u_i + \Theta_i\end{aligned} \tag{3}$$

where $p_i = [x_i, y_i, z_i]^T$, $\Gamma_i = -\mathrm{diag}[K_1/m_i, K_2/m_i, K_3/m_i]$, $\Theta_i = [d_{i,1}, d_{i,2}, d_{i,3}]^T$, and position control input $u_i = [u_{i,x}, u_{i,y}, u_{i,z}]^T$. Based on this outer loop dynamic, the position control input $u_i$ can be designed. Subsequently, the desired attitude for the inner loop can be generated by using a standard function and the designed position control input [57,60].

$$\begin{aligned}T_{i,z} &= m\sqrt{u_{i,x}^2 + u_{i,y}^2 + (u_{i,z} + g)^2}\\ \varphi_{i,d} &= \arcsin\left(m_i \tfrac{u_{i,x}S(\psi_{i,d}) - u_{i,y}C(\psi_{i,d})}{T_{i,z}}\right)\\ \theta_{i,d} &= \arctan\left(\tfrac{u_{i,x}C(\psi_{i,d}) + u_{i,y}S(\psi_{i,d})}{u_{i,z}+g}\right)\end{aligned} \tag{4}$$

where $\psi_{i,d}$ is the desired yaw angle that can be specified independently in advance. In this paper, we mainly focus on outer loop safety-critical control and assume that there exists an attitude control law for tracking the desired attitude obtained by outer loop control.

### 2.2. Graph Theory

The communication of this multi-agent system (MAS) is described by an undirected graph $\mathcal{G} = (\mathcal{V}, \mathcal{E})$, where $\mathcal{V} = \{m_1, \ldots, m_N\}$ is the node set and $\mathcal{E} \subseteq \{(m_i, m_k) | m_i, m_k \in \mathcal{V}, m_i \neq m_k\}$ represents the edge set. The correlation adjacency matrix $\mathcal{A} = [a_{ik}]$ is determined as $a_{ik} = 1$ if the $i$-th UAV is capable of receiving information from the $k$-th UAV; otherwise, $a_{ik} = 0$. We consider $N_i = \{m_k | (m_i, m_k) \in E\}$ as the neighbor set of $m_i$. The Laplacian matrix $L$ is defined by $L = [l_{ik}] \in \mathbb{R}^{n\times n}$, where $l_{ii} = \sum_{k\in\mathcal{N}_i} a_{ik}$, $l_{ik} = -a_{ik}$.

### 2.3. Control Objectives

*Fixed-time formation control:* We aim to design a control strategy to ensure that follower UAVs track the leader in a fixed time.

*Safety guarantee and obstacle avoidance:* We aim to ensure that all UAVs can avoid collisions with stationary and moving obstacles in the environment.

### *2.4. Necessary Lemmas and Assumptions*

**Lemma 1 [61].** *Consider the following system*

$$\dot{x} = f(x),\ x(0) = x_0,\ x \in \mathbb{R}^n \tag{5}$$

*If there exists a function satisfying*

$$\dot{V}(x) \leq -aV^m(x) - bV^n(x) \tag{6}$$

*where $a > 0$, $b > 0$, $0 < m < 1$, and $n > 1$, we can obtain a system (5) which is fixed-time stable, with the stable time bounded by*

$$T \leq \frac{1}{a(1-m)} + \frac{1}{b(n-1)} \tag{7}$$

**Lemma 2 [62].** *For constants $c_i \geq 0$, if $0 < m < 1$, we have*

$$\sum_{i=1}^{k} c_i^m \geq \left(\sum_{i=1}^{k} c_i\right)^m \tag{8}$$

*and if $m > 1$, we have*

$$\sum_{i=1}^{k} c_i^m \geq n^{1-m}\left(\sum_{i=1}^{k} c_i\right)^m \tag{9}$$

**Assumption 1.** *For each follower UAV, there exists at least one path to the leader.*

**Assumption 2.** *The acceleration of the leader is bounded and satisfies $\|\dot{v}_0\| \leq \rho$.*

## 3. Nominal Formation Control Law

### *3.1. Fixed-Time Disturbance Observer*

To design the formation control law, the dynamics of the model are needed. However, the disturbances caused by air currents are unavoidable. We provide a fixed-time DO to estimate these disturbances:

$$\begin{aligned}
&\mu_i = v_i - \hat{v}_i \\
&\dot{\hat{v}}_i = u_i + \Gamma_i v_i + \hat{\Theta}_i \\
&s_i = \dot{\mu}_i + \kappa_{1,i}\wp_i \\
&\dot{\wp}_i = \kappa_{2,i}\mathrm{sig}(\dot{\mu}_i)^{n_1} + \kappa_{3,i}\mathrm{sig}(\dot{\mu}_i)^{n_2} \\
&\dot{\hat{\Theta}}_i = \kappa_{1,i}\dot{\wp}_i + \eta_{1,i}\mathrm{sig}(s_i)^{n_1} + \eta_{2,i}\mathrm{sig}(s_i)^{n_2} + \eta_{3,i}\mathrm{sign}(s_i)
\end{aligned} \tag{10}$$

where $\hat{\Theta}_i$ and $\hat{v}_i$ are the estimates for $\Theta_i$ and $v_i$, respectively. $\kappa_{1,i}$, $\kappa_{2,i}$, $\kappa_{3,i}$, $\eta_{1,i}$, $\eta_{2,i}$, and $\eta_{3,i}$ are positive constants, with $\left\|\dot{\Theta}_i\right\| \leq \eta_{3,i}$, $0 < n_1 < 1$, and $n_2 > 1$. The function $\mathrm{sig}(\bullet)^a$ can be defined as $\mathrm{sig}(m)^a = |m|^a \mathrm{sign}(m)$, with $\mathrm{sign}(\bullet)$ being the signum function. The $\mu_i$, $s_i$, and $\wp_i$ are the state variables of this observer.

Note that the velocity of the UAV is accessible in this work, and the reason for its estimation in (10) is the need for the observer design; in other words, we can consider it a state variable in this observer. Then, we present the following conclusion.

**Lemma 3.** *Considering the dynamic model (3) with external disturbance, the fixed-time DO (10) can estimate disturbances, with the error of the estimate converging to zero in a fixed time.*

**Proof.** Considering the Lyapunov function $V = \frac{1}{2}s_i^T s_i$, its derivative can be given by

$$\begin{aligned}
\dot{V} &= s_i^T(\dot{\Theta}_i - \dot{\hat{\Theta}}_i + \kappa_{1,i}\dot{\wp}_i) \\
&= s_i^T\dot{\Theta}_i - \eta_{1,i}s_i^T\mathrm{sig}(s_i)^{n_1} - \eta_{2,i}s_i^T\mathrm{sig}(s_i)^{n_2} - \eta_{3,i}s_i^T\mathrm{sign}(s_i) \\
&\leq -\eta_{1,i}s_i^T\mathrm{sig}(s_i)^{n_1} - \eta_{2,i}s_i^T\mathrm{sig}(s_i)^{n_2} \\
&\leq -\eta_{1,i}|s_i|^{n_1+1} - \eta_{2,i}|s_i|^{n_2+1} \\
&\leq -2^{(n_1+1)/2}\eta_{1,i}V^{(n_1+1)/2} - 2^{(n_2+1)/2}\eta_{2,i}V^{(n_2+1)/2}
\end{aligned} \tag{11}$$

where the first inequality comes from $s_i^T\dot{\Theta}_i - \eta_{3,i}s_i^T\text{sign}(s_i) \leq \|s_i\|_1\left\|\dot{\Theta}_i\right\|_2 - \eta_{3,i}\|s_i\|_1 \leq 0$. According to Lemma 1, $s_i$ will converge to zero within a fixed time

$$t_1 \leq \frac{2}{2^{(n_1+1)/2}\eta_{1,i}(1-n_1)} + \frac{2}{2^{(n_2+1)/2}\eta_{2,i}(n_2-1)} \tag{12}$$

Thus, we can get $\dot{\mu}_i = -\kappa_{1,i}\wp_i$, which implies that

$$\begin{aligned}\dot{\wp}_i &= \kappa_{2,i}\text{sig}(\dot{\mu}_i)^{n_1} + \kappa_{3,i}\text{sig}(\dot{\mu}_i)^{n_2} \\ &= -\kappa_{2,i}\kappa_{1,i}^{n_1}\text{sig}(\wp_i)^{n_1} - \kappa_{3,i}\kappa_{1,i}^{n_2}\text{sig}(\wp_i)^{n_2}\end{aligned} \tag{13}$$

Therefore, by considering $V = \frac{1}{2}\wp_i^T\wp_i$ and following the preceding proof, we can conclude that $\wp_i$ will converge to zero within a fixed time

$$t_2 \leq \frac{2}{2^{(n_1+1)/2}\kappa_{2,i}\kappa_{1,i}^{n_1}(1-n_1)} + \frac{2}{2^{(n_2+1)/2}\kappa_{3,i}\kappa_{1,i}^{n_2}(n_2-1)} \tag{14}$$

Since the estimation error $\widetilde{\Theta}_i = \Theta_i - \hat{\Theta}_i = \dot{\mu}_i = -\kappa_{1,i}\wp_i$, $\wp_i$ converges to zero, which implies that $\widetilde{\Theta}_i$ converges to zero within a fixed time

$$T \leq \frac{2}{2^{(n_1+1)/2}\eta_{1,i}(1-n_1)} + \frac{2}{2^{(n_2+1)/2}\eta_{2,i}(n_2-1)} + \frac{2}{2^{(n_1+1)/2}\kappa_{2,i}\kappa_{1,i}^{n_1}(1-n_1)} + \frac{2}{2^{(n_2+1)/2}\kappa_{3,i}\kappa_{1,i}^{n_2}(n_2-1)} \tag{15}$$

The proof has ended. □

### *3.2. Nominal Control Law*

In Section 3.1, we present a fixed-time DO that will be used to deal with external disturbances. Based on this, we propose a fixed-time nominal control law in this section.

Since the control law is distributed, not every UAV can access the leader's state information. Thus, we first propose a fixed-time distributed observer, which can estimate the leader's position and velocity simultaneously.

$$\begin{aligned}\dot{\chi}_i &= -k_1\text{sig}\left(\textstyle\sum_{j=0}^N a_{ij}(\chi_i-\chi_j)\right)^{a_1/a_2} - k_2\text{sig}\left(\textstyle\sum_{j=0}^N a_{ij}(\chi_i-\chi_j)\right)^{b_1/b_2} + \varsigma_i \\ \dot{\varsigma}_i &= -k_1\text{sig}\left(\textstyle\sum_{j=0}^N a_{ij}(\varsigma_i-\varsigma_j)\right)^{a_1/a_2} - k_2\text{sig}\left(\textstyle\sum_{j=0}^N a_{ij}(\varsigma_i-\varsigma_j)\right)^{b_1/b_2} - k_3\text{sign}\left(\textstyle\sum_{j=0}^N a_{ij}(\varsigma_i-\varsigma_j)\right)\end{aligned} \tag{16}$$

where $\chi_i$ and $\varsigma_i$ are the $i$-th follower's estimate for $p_0$ and $v_0$, respectively. $k_1 > 0$, $k_2 > 0$, and $k_3 > \rho$ are the observer gains, and $a_1$, $a_2$, $b_1$, and $b_2$ are positive constants that satisfy $a_1 > a_2$ and $b_1 < b_2$.

**Lemma 4.** *If Assumptions 1 and 2 are held, the distributed observer (16) can estimate the leader's position and velocity simultaneously in a fixed time, i.e., $\chi_i \to p_0$ and $\varsigma_i \to v_0$ as*

$$t \leq \frac{2a_2}{k_1 N^{\frac{1-a_1/a_2}{2}}\lambda_{\min}(H)(a_1-a_2)} + \frac{2b_2}{k_2\lambda_{\min}(H)(b_2-b_1)} \tag{17}$$

*with matrix $H = L_F + B$, where $L_F$ is the Laplacian matrix of followers' subgraph and $B = \text{diag}\{a_{10},\ldots,a_{N0}\}$.*

**Proof.** We first define the error of the estimate as $\widetilde{\chi}_i = \chi_i - p_0$ and $\widetilde{\varsigma}_i = \varsigma_i - v_0$; then we can get

$$\begin{aligned}\dot{\widetilde{\chi}}_i &= -k_1\text{sig}\left(\textstyle\sum_{j=0}^N a_{ij}(\widetilde{\chi}_i-\widetilde{\chi}_j)\right)^{a_1/a_2} - k_2\text{sig}\left(\textstyle\sum_{j=0}^N a_{ij}(\widetilde{\chi}_i-\widetilde{\chi}_j)\right)^{b_1/b_2} + \widetilde{\varsigma}_i \\ \dot{\widetilde{\varsigma}}_i &= -k_1\text{sig}\left(\textstyle\sum_{j=0}^N a_{ij}(\widetilde{\varsigma}_i-\widetilde{\varsigma}_j)\right)^{a_1/a_2} - k_2\text{sig}\left(\textstyle\sum_{j=0}^N a_{ij}(\widetilde{\varsigma}_i-\widetilde{\varsigma}_j)\right)^{b_1/b_2} - k_3\text{sign}\left(\textstyle\sum_{j=0}^N a_{ij}(\widetilde{\varsigma}_i-\widetilde{\varsigma}_j)\right) - \dot{v}_0\end{aligned} \tag{18}$$

We consider the Lyapunov function $V = \frac{1}{2}\widetilde{\varsigma}^T H \widetilde{\varsigma}$, where $\widetilde{\varsigma} = [\widetilde{\varsigma}_1^T, \ldots, \widetilde{\varsigma}_N^T]^T$. Moreover, according to the symmetry of $H$, we can further get

$$\frac{dV}{d\widetilde{\varsigma}_i} = \sum_{j=0}^{N} a_{ij}(\widetilde{\varsigma}_i^T - \widetilde{\varsigma}_i^T) \tag{19}$$

Therefore, we can calculate $\dot{V}$ as

$$\begin{aligned}
\dot{V} &= \sum_{i=1}^{N}\left(\sum_{j=0}^{N} a_{ij}(\widetilde{\varsigma}_i^T - \widetilde{\varsigma}_j^T)\dot{\widetilde{\varsigma}}_i\right) \\
&\leq \sum_{i=1}^{N}\left(-k_1\left|\sum_{j=0}^{N} a_{ij}\left(\varsigma_i - \varsigma_j\right)\right|^{a_1/a_2+1} - k_2\left|\sum_{j=0}^{N} a_{ij}(\widetilde{\varsigma}_i^T - \widetilde{\varsigma}_j^T)\right|^{b_1/b_2+1} - (k_3-\rho)\left\|\sum_{j=0}^{N} a_{ij}(\widetilde{\varsigma}_i^T - \widetilde{\varsigma}_j^T)\right\|_1\right) \\
&\leq -k_1\sum_{i=1}^{N}\left(\left\|\sum_{j=0}^{N} a_{ij}(\widetilde{\varsigma}_i - \widetilde{\varsigma}_j)\right\|^2\right)^{\frac{a_1/a_2+1}{2}} - k_2\sum_{i=1}^{N}\left(\left\|\sum_{j=0}^{N} a_{ij}(\widetilde{\varsigma}_i - \widetilde{\varsigma}_j)\right\|^2\right)^{\frac{b_1/b_2+1}{2}} \\
&\leq -k_1 N^{\frac{1-a_1/a_2}{2}}\left(\sum_{i=1}^{N}\left(\left\|\sum_{j=0}^{N} a_{ij}\left(\varsigma_i - \varsigma_j\right)\right\|^2\right)\right)^{\frac{a_1/a_2+1}{2}} - k_2\left(\sum_{i=1}^{N}\left(\left\|\sum_{j=0}^{N} a_{ij}(\widetilde{\varsigma}_i^T - \widetilde{\varsigma}_j^T)\right\|^2\right)\right)^{\frac{b_1/b_2+1}{2}}
\end{aligned} \tag{20}$$

where the last inequality comes from Lemma 2. Also, since the matrix $H$ is positive-definite, we can get the following inequality

$$\sum_{i=1}^{N}\left(\left\|\sum_{j=0}^{N} a_{ij}(\widetilde{\varsigma}_i - \widetilde{\varsigma}_j)\right\|^2\right) = \widetilde{\varsigma}^T H^T H \widetilde{\varsigma} \geq 2\lambda_{\min}(H) \times V \tag{21}$$

Thus, letting $\overline{V} = \sqrt{2\lambda_{\min}(H)V}$ and combining this with (20) and (21), we can obtain

$$\dot{\overline{V}} = -k_1 N^{\frac{1-a_1/a_2}{2}}\lambda_{\min}(H)\overline{V}^{a_1/a_2} - k_2\lambda_{\min}(H)\overline{V}^{b_1/b_2} \tag{22}$$

Then, according to Lemma 1, we conclude that $\overline{V}$ and $V$ can converge to zero in a fixed time, i.e., $\widetilde{\varsigma}_i \to 0$ as

$$t \leq \frac{a_2}{k_1 N^{\frac{1-a_1/a_2}{2}}\lambda_{\min}(H)(a_1 - a_2)} + \frac{b_2}{k_2\lambda_{\min}(H)(b_2 - b_1)}$$

In this way, we can obtain

$$\dot{\widetilde{\chi}}_i = -k_1 \mathrm{sig}\left(\sum_{j=0}^{N} a_{ij}\left(\widetilde{\chi}_i - \widetilde{\chi}_j\right)\right)^{a_1/a_2} - k_2 \mathrm{sig}\left(\sum_{j=0}^{N} a_{ij}\left(\widetilde{\chi}_i - \widetilde{\chi}_j\right)\right)^{b_1/b_2}$$

Then, we consider the Lyapunov function $V = \frac{1}{2}\widetilde{\chi}^T H \widetilde{\chi}$, where $\widetilde{\chi} = [\widetilde{\chi}_1^T, \ldots, \widetilde{\chi}_N^T]^T$. Thus, the following process can be in line with the above, and we can conclude that $\widetilde{\chi}_i \to 0$ and $\widetilde{\varsigma}_i \to 0$ within a fixed time given in (17). The proof has ended. □

Then, tracking error for the $i$-th follower is given by $z_{1,i} = p_i - \chi_i - p_i^*$, where $p_i^*$ denotes the formation configuration, i.e., the relative position between the $i$-th follower and the leader. The derivative of $z_{1,i}$ can be given by $\dot{z}_{1,i} = \nu_i - \varsigma_i$. Thus, we design the virtual control law as

$$\alpha_i = -k_{1,i} z_{1,i} - \gamma_1 \mathrm{sig}^{2-m_1/m_2}(z_{1,i}) - \gamma_2 \mathrm{sig}^{m_1/m_2}(z_{1,i}) + \varsigma_i \tag{23}$$

where $k_{1,i} > 0$, $\gamma_1 > 0$, $\gamma_2 > 0$, and $m_2 > m_1 > 0$. Furthermore, we consider the velocity tracking error as $z_{2,i} = v_i - \alpha_i$, whose derivative can be computed as

$$\dot{z}_{2,i} = \Gamma_i v_i + u_i + \Theta_i - \dot{\alpha}_i \tag{24}$$

Then, we provide the following nominal control law:

$$u_i = -k_{2,i} z_{2,i} - z_{1,i} - \gamma_1 \mathrm{sig}^{2-m_1/m_2}(z_{2,i}) - \gamma_2 \mathrm{sig}^{m_1/m_2}(z_{2,i}) + \dot{\alpha}_i - \hat{\Theta}_i - \Gamma_i v_i \tag{25}$$

where $k_{2,i} > 0$, and $\hat{\Theta}_i$ is the estimate of external disturbance obtained from the fixed-time disturbance observer (10). The block diagram of the proposed control law is shown in Figure 1. Thus, we present the following conclusion.

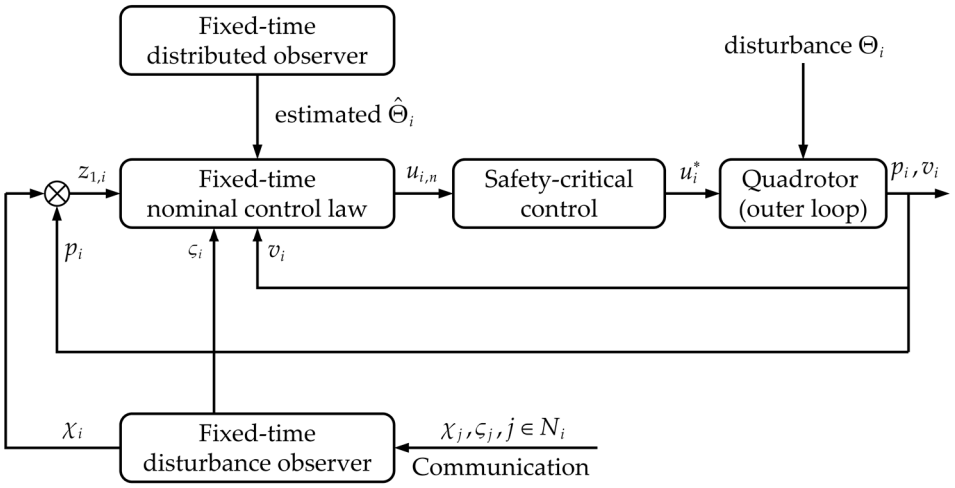


**Figure 1.** Block diagram of the control law.

**Theorem 1.** *Consider a MAS with a virtual leader and N followers modeled by (3). Under the distributed observer (16), fixed-time disturbance observer (10), and control law (25), all followers can track the leader, with tracking error converging to zero in a fixed time.*

**Proof.** Consider the following Lyapunov function

$$V_i = \frac{1}{2} z_{1,i}^T z_{1,i} + \frac{1}{2} z_{2,i}^T z_{2,i} \tag{26}$$

We calculate the derivative of $V$ as

$$\begin{aligned}
\dot{V}_i &= z_{1,i}^T \left( -k_{1,i} z_{1,i} - \gamma_1 \mathrm{sig}^{2-m_1/m_2}(z_{1,i}) - \gamma_2 \mathrm{sig}^{m_1/m_2}(z_{1,i}) + z_{2,i} \right) \\
&\quad + z_{2,i}^T \left( -k_{2,i} z_{2,i} - z_{1,i} - \gamma_1 \mathrm{sig}^{2-m_1/m_2}(z_{2,i}) - \gamma_2 \mathrm{sig}^{m_1/m_2}(z_{2,i}) + \widetilde{\Theta}_i \right) \\
&= -k_{1,i} z_{1,i}^T z_{1,i} - k_{2,i} z_{2,i}^T z_{2,i} + z_{2,i}^T \widetilde{\Theta}_i \\
&\quad - \gamma_1 \left( |z_{1,i}|^{3-m_1/m_2} + |z_{2,i}|^{3-m_1/m_2} \right) - \gamma_2 \left( |z_{1,i}|^{1+m_1/m_2} + |z_{2,i}|^{1+m_1/m_2} \right) \\
&\le -\gamma_1 \left( \left( z_{1,i}^T z_{1,i} \right)^{\frac{3m_2-m_1}{2m_2}} + \left( z_{2,i}^T z_{2,i} \right)^{\frac{3m_2-m_1}{2m_2}} \right) - \gamma_2 \left( \left( z_{1,i}^T z_{1,i} \right)^{\frac{m_1+m_2}{2m_2}} + \left( z_{2,i}^T z_{2,i} \right)^{\frac{m_1+m_2}{2m_2}} \right) + \varepsilon_i \\
&\le -2\gamma_1 V_i^{\frac{3m_2-m_1}{2m_2}} - \gamma_2 2^{\frac{m_1+m_2}{2m_2}} V_i^{\frac{m_1+m_2}{2m_2}} + \varepsilon_i
\end{aligned} \tag{27}$$

where $\varepsilon_i = \|z_{2,i}\|_2 \left\| \widetilde{\Theta}_i \right\|_2$, and the last inequality comes from Lemma 2. Based on Lemma 6 in [63], we can conclude that $z_{1,i}$ and $z_{2,i}$ will converge to a compact set

$$Q = \left\{ z_{1,i}, z_{2,i} | V_i \le \min \left\{ \left( \frac{\varepsilon_i}{2\gamma_1 (1-\omega_i)} \right)^{\frac{2m_2}{3m_2-m_1}}, \left( \frac{\varepsilon_i}{2^{\frac{m_1+m_2}{2m_2}} \gamma_2 (1-\omega_i)} \right)^{\frac{m_1+m_2}{2m_2}} \right\} \right\} \tag{28}$$

in a fixed time

$$t \le \frac{2m_2}{\gamma_1 \omega_i 2^{\frac{3m_2-m_1}{2m_2}} (m_2 - m_1)} + \frac{2m_2}{\gamma_2 \omega_i 2^{\frac{m_1+m_2}{2m_2}} (m_2 - m_1)} \tag{29}$$

The proof has ended. □

## 4. Safety-Critical Control via CBF

### *4.1. Control Barrier Functions*

In Section 3, we provide a nominal fixed-time control law to ensure that UAVs can track the leader. However, obstacle avoidance should be considered during the tracking process. Moreover, tracking performance should be guaranteed to the extent possible when avoiding obstacles; i.e., the nominal control law should be modified as little as possible. In this section, we achieve these goals by using an optimization-based control approach.

We first provide the definition of CBFs, which will be applied to construct the safety constraints for optimization programs. We first rewrite (3) as

$$\dot{\boldsymbol{x}}_i = f(\boldsymbol{x}_i) + g(\boldsymbol{x}_i)u_i \tag{30}$$

where

$$\dot{\boldsymbol{x}}_i = \mathrm{col}(p_i, v_i), f(\boldsymbol{x}_i) = \begin{bmatrix} v_i \\ \Gamma_i v_i + \Theta_i \end{bmatrix}, g(\boldsymbol{x}_i) = \begin{bmatrix} 0_{3\times 3} \\ I_{3\times 3} \end{bmatrix}$$

Then, we define a superlevel safety set for the state $\boldsymbol{x}_i$

$$C = \{\boldsymbol{x}_i \in \mathbb{R}^n | h(\boldsymbol{x}_i) \geq 0\} \tag{31}$$

where $h(\boldsymbol{x}_i)$:$\mathbb{R}^n \to \mathbb{R}$ is a smooth function. In the context of obstacle avoidance, the function $h(\boldsymbol{x}_i)$ can be designed as

$$h(\boldsymbol{x}_i) = (p_i - p_{ob})^T (p_i - p_{ob}) - d_{ob}^2 \tag{32}$$

where $p_{ob} = [x_{ob}, y_{ob}, z_{ob}]^T$ is the obstacle's position, and $d_{ob}$ denotes the safety distance. Thus, obstacle avoidance can be guaranteed by ensuring the forward invariance of the safety set (31). Then, we present the following definition of CBF.

**Definition 1 [43].** *Given the safety set C defined in (31), $h(\boldsymbol{x})$ is a CBF if there exists an extended class $K_\infty$ function $\alpha$ such that*

$$\sup_{u\in U}[L_f h(\boldsymbol{x}) + L_g h(\boldsymbol{x})u] \geq -\alpha(h(\boldsymbol{x})) \tag{33}$$

*where $L_f h(\boldsymbol{x}) = [\partial h(\boldsymbol{x})/\partial \boldsymbol{x}] f(\boldsymbol{x})$ and $L_g h(\boldsymbol{x}) = [\partial h(\boldsymbol{x})/\partial \boldsymbol{x}] g(\boldsymbol{x})$ denotes the Lie derivative. We note that (33) seems to provide a safety constraint for u, which can be used in the optimization. In fact, an important premise is that $L_g h(\boldsymbol{x}) \neq \mathbf{0}$; i.e., $h(\boldsymbol{x})$ has a relative degree of one [64]. We can see that the optimization variable u will vanish if $L_g h(\boldsymbol{x}) = \mathbf{0}$.*

However, calculations show that $L_g h(\boldsymbol{x}) = \mathbf{0}$ for our proposed CBF (32) since this CBF is position-based and the optimization variable is force/torque. To address this problem, we further introduce the exponential control barrier functions (ECBFs), which can ensure the forward invariance of set (31) for arbitrary relative-degree systems.

**Definition 2 [64].** *Given a safety set as defined in (31), in which; $h(\boldsymbol{x})$ is an r-times differentiable function, $h(\boldsymbol{x})$ is an ECBF if there exists a $\Pi \in \mathbb{R}^{1\times r}$ such that*

$$\sup_{u\in U}[L_f^r h(\boldsymbol{x}) + L_g L_f^{r-1} h(\boldsymbol{x})u] \geq -\Pi\theta(\boldsymbol{x}) \tag{34}$$

*where $\theta(\boldsymbol{x}) = [h, h^{(1)}, \ldots, h^{(r-1)}]^T = [h(\boldsymbol{x}), L_f h(\boldsymbol{x}), \ldots, L_f^{r-1} h(\boldsymbol{x})]^T$. Meanwhile, a systematic procedure is introduced to determine the $\Pi$, and we first consider a virtual control input as follows*

$$\xi = L_f^r h(\boldsymbol{x}) + L_g L_f^{r-1} h(\boldsymbol{x})u \tag{35}$$

*In this way, we can get the following input–output linear system model*

$$\begin{aligned} \dot{\theta}(\boldsymbol{x}) &= M\theta(\boldsymbol{x}) + N\xi \\ h(\boldsymbol{x}) &= F\theta(\boldsymbol{x}) \end{aligned} \tag{36}$$

*with*

$$M = \begin{pmatrix} 0 & 1 & 0 & \cdots & 0 \\ 0 & 0 & 1 & \cdots & 0 \\ \vdots & \vdots & \vdots & \ddots & \vdots \\ 0 & 0 & 0 & \cdots & 1 \\ 0 & 0 & 0 & \cdots & 0 \end{pmatrix} \in \mathbb{R}^{r\times r}, N = \begin{pmatrix} 0 \\ 0 \\ \vdots \\ 0 \\ 1 \end{pmatrix} \in \mathbb{R}^{r}, F = [1\,0\cdots 0\,0] \in \mathbb{R}^{1\times r} \tag{37}$$

*We note that (36) is a controllable canonical form; then, we can use the pole placement lemma to regularize this system. In other words, if we design a* $\xi$ *such that it satisfies* $\xi \geq -\Pi\theta(\boldsymbol{x})$ *with* $M - N\Pi$ *being Hurwitz and total negative, then we can conclude that* $h(\boldsymbol{x}) \geq Fe^{(M-N\Pi)t}\theta(\boldsymbol{x}(0)) \geq 0$ *holds with* $h(\boldsymbol{x}_0) \geq 0$*. In this way, the forward invariance of the safety set can be ensured. We first denote* $\lambda_a = -[\lambda_1, \ldots, \lambda_r]$ *as the eigenvalues of* $M - N\Pi$*; then, we introduce a family of functions and their sets as*

$$\begin{aligned} &y_i(\boldsymbol{x}) = \dot{y}_{i-1}(\boldsymbol{x}) + \lambda_i y_{i-1}(\boldsymbol{x}), i = 1, \ldots, r \\ &C_i = \{\boldsymbol{x} \in \mathbb{R}^n | y_i(\boldsymbol{x}) \geq 0\}, \end{aligned} \tag{38}$$

*where* $y_0(\boldsymbol{x}) = h(\boldsymbol{x})$*. Then, we can present the following conclusion.*

**Theorem 2 [64].** $\xi \geq -\Pi\theta(\boldsymbol{x})$ *ensures that* $h(\boldsymbol{x})$ *is an ECBF if* $\Pi$ *is designed such that* $\lambda_i > 0$ *and* $-\lambda_i \geq -\dot{y}_{i-1}(\boldsymbol{x}_0)/y_{i-1}(\boldsymbol{x}_0)$, $i = 1, \ldots, r$.

Given a proper $\Pi$ satisfying the conditions in Theorem 2, control input in (34) will ensure the forward invariance of the safety set (31), and therefore, no collision occurs. Thus, we can formulate a QP using (34) as a constraint to optimize the nominal control law proposed in Section 3.

$$\begin{aligned} &u^* = \text{argmin}_{u\in U}\|u - u_n\|^2 \\ &\text{s.t.}\xi \geq -\Pi\theta(\boldsymbol{x}),\ \xi = L_f^r h(\boldsymbol{x}) + L_g L_f^{r-1} h(\boldsymbol{x})u \end{aligned} \tag{39}$$

where $u_n$ denotes the nominal formation tracking control law proposed in (25).

**Remark 1.** *We can see that the ECBF guarantees the forward invariance of the safety set by introducing a virtual control input and using an input–output feedback control approach. In this process, the pole placement lemma provides a standard method for designing the parameters in ECBFs.*

**Remark 2.** *Note that the actual control law (39) is worked out via a quadratic program subject to safety constraints established using ECBFs, which is closest to the nominal control law (25) and satisfies safety constraints at the same time. Therefore, tracking performance is minimally affected while achieving collision-free behavior.*

### *4.2. Robust ECBF Design*

In Section 4.1, we provide the ECBFs that are used to optimize the nominal control law and ensure that no collision occurs. However, we note that accurate dynamic model information is needed in safety constraints; i.e., $f(\boldsymbol{x})$ contains external disturbances $\Theta_i$ that are unknown. In order to address this problem, we provide a robust ECBF in this section to construct robust safety constraints despite external disturbances.

For system (30) and $h(\boldsymbol{x})$ designed in (32), calculations show that $L_g h(\boldsymbol{x}) = \mathbf{0}$ and $L_g L_f h(\boldsymbol{x}) \neq \mathbf{0}$. Then, we conclude that $h(\boldsymbol{x})$ has a relative degree of two. Based on this and taking disturbance into account, the virtual control input in (35) can be written as

$$\begin{aligned} \xi &= L_{\overline{f}}^2 h(\boldsymbol{x}) + L_g L_f h(\boldsymbol{x}) u \\ &= L_{\overline{f}}^2 h(\boldsymbol{x}) + L_g L_{\overline{f}} h(\boldsymbol{x}) u + \delta_1 + \delta_2 [L_{\overline{f}}^2 h(\boldsymbol{x}) + L_g L_{\overline{f}} h(\boldsymbol{x}) u] \\ &= \overline{\xi} + \delta_1 + \delta_2 \overline{\xi} \end{aligned} \tag{40}$$

where $\overline{f}(\boldsymbol{x}) = \mathrm{col}(v_i, \Gamma_i v_i)$ is the term without considering disturbances, $\delta_1$ and $\delta_2$ are the uncertain terms caused by the difference between $\overline{f}(\boldsymbol{x})$ and $f(\boldsymbol{x})$, i.e., the disturbances, and $\overline{\xi} = L_{\overline{f}}^2 h(\boldsymbol{x}) + L_g L_{\overline{f}} h(\boldsymbol{x}) u$. Suppose that $|\delta_1| \leq \delta_1^*$ and $|\delta_2| \leq \delta_2^*$; the safety constraints can be rewritten as

$$\begin{aligned} &\min \ \overline{\xi} + \delta_1 + \delta_2 \overline{\xi} \geq -\Pi \theta(\boldsymbol{x}), \\ &|\delta_1| \leq \delta_1^*, \ |\delta_2| \leq \delta_2^* \end{aligned} \tag{41}$$

Based on this, in order to compute the $\overline{\xi}$ satisfying (41) for all $|\delta_1| \leq \delta_1^*$, $|\delta_2| \leq \delta_2^*$, we design the following robust constraints

$$\Phi + \Xi_1 \overline{\xi} \geq 0, \ \Phi + \Xi_2 \overline{\xi} \geq 0 \tag{42}$$

where $\Phi = \Pi \theta(\boldsymbol{x}) - \delta_1^*$, $\Xi_1 = 1 + \delta_2^*$, and $\Xi_2 = 1 - \delta_2^*$. Therefore, we can present the following conclusion.

**Theorem 3.** *Considering multiple UAVs modeled by (3), with the nominal fixed-time control law (25) and the safety set (31), obstacle avoidance can be achieved using the safety-critical fixed-time control input solved by the following QP*

$$\begin{aligned} &u_i^* = \mathrm{argmin}_{u_i \in U} \|u_i - u_{i,n}\|^2 \\ &\text{s.t.} \Phi_i + \Xi_{1,i} \overline{\xi}_i \geq 0, \ \Phi_i + \Xi_{2,i} \overline{\xi}_i \geq 0 \\ &\overline{\xi}_i = L_{\overline{f}}^2 h(\boldsymbol{x}_i) + L_g L_{\overline{f}} h(\boldsymbol{x}_i) u_i \end{aligned} \tag{43}$$

*where* $L_{\overline{f}}^2 h(\boldsymbol{x}_i) = 2 v_i^T v_i + 2(q_i - q_{ob})^T \Gamma_i v_i$, $L_g L_{\overline{f}} h(\boldsymbol{x}_i) = 2(q_i - q_{ob})^T$, *and* $u_{i,n}$ *is the nominal control input in (25).*

**Proof.** The control input solved by the QP meets the safety conditions in (43), which are constructed using robust ECBFs. From the above analysis, it can ensure the forward invariance of safety set (31), and thus, the $h(\boldsymbol{x}_i) \geq 0$ for all time. Then, according to the definition of $h(\boldsymbol{x}_i)$ in (32), collision avoidance is achieved. □

## 5. Simulation

We provide simulations to test the validity of the proposed method, based on a MAS with one virtual leader and four UAV followers. The dynamic model we used is same as that in [65]. With leader being labeled 0 and the followers being labeled 1, 2, 3, and 4, the communication topology is defined as (0, 1), (0, 2), (1, 3), (2, 3), (2, 4). The trajectory of the leader is $p_0 = [60 + 25\cos(-0.06t + \pi), 60 + 25\sin(-0.06t + \pi), 0.5t]^T$ m, and the desired relative positions are $p_1^* = [-3, 3, 0]^T$ m, $p_2^* = [-3, -3, 0]^T$ m, $p_3^* = [3, 3, 0]^T$ m, and $p_4^* = [3, -3, 0]^T$ m. The initial states of the UAVs are $p_1 = [30, 65, 3]^T$ m, $p_2 = [31, 56, -4]^T$ m, $p_3 = [39, 66, 2]^T$ m, $p_4 = [41, 57, -3]^T$ m, and $v_i = [0.1, -0.15, 0.17]^T$ m/s. Five stationary obstacles and one moving obstacle are introduced to pose six collision threats, with $p_{ob,1} = [47, 86, 10]^T$ m, $p_{ob,2} = [52, 78, 9]^T$ m, $p_{ob,3} = [43, 82, 61.5]^T$ m, $p_{ob,4} = [49, 75, 60.5]^T$ m, $p_{ob,5} = [95 - 0.06t, 15 + 0.001 \times t^2, 100 - 0.089t]^T$ m, $p_{ob,6} = [69, 83, 124.5]^T$ m, $d_{ob,1} = 5$ m, $d_{ob,2} = 4$ m, $d_{ob,3} = 5$ m, $d_{ob,4} = 5.5$ m, $d_{ob,5} = 3$ m, and $d_{ob,6} = 6$ m. The control parameters are set as $k_{1,i} = 2$, $k_{2,i} = 3$, $\gamma_1 = \gamma_2 = 0.5$, $m_1 = 1$, and $m_2 = 2$. The parameters in the DO are set as $\kappa_{1,i} = 4$, $\kappa_{2,i} = 2$, $\kappa_{3,i} = 3$, $\varpi_{1,i} = 1.5$, $\varpi_{2,i} = 1.5$, $\varpi_{3,i} = 0.5$, $n_1 = 0.5$, and $n_2 = 1.5$.

Figures 2–6 show the simulation results. Figure 2 shows the tracking paths of the four followers guided by one virtual leader using the proposed safety-critical fixed-time formation control law. We see that the UAV followers track the leader and form the desired formation despite disturbances. Meanwhile, collision avoidance with five stationary obstacles and one moving obstacle is achieved. Figure 3 shows four snapshots from the obstacle avoidance process. We can see that UAV-1 and UAV-3 go around the stationary obstacle-1 during 15~35 s; at the same time, UAV-4 avoids the stationary obstacle-2, UAV-1, UAV-2, and UAV-3 bypass the stationary obstacle-3 during 115~137 s, and UAV-4 avoids stationary obstacle-4 during 117~134 s. The moving obstacle is avoided by UAV-4 during 167~182 s, and all UAVs bypass the last stationary obstacle during 240~268 s. Moreover, we note that the obstacle avoidance behavior is only enforced when collision is truly imminent, which guarantees that tracking performance is minimally affected. Figure 4 illustrates the tracking errors of the UAVs, with the area marked in red corresponding to the period when obstacle avoidance occurs. We can see that the tracking errors converge to 0 in a fixed time when there is no obstacle threat, which verifies the usefulness of the nominal control law. Figure 5 illustrates the $h(\boldsymbol{x})$ defined in (32), which visually demonstrates that the safety constraints are not violated, and obstacle avoidance behavior is achieved. Figure 6 illustrates the optimized actual control inputs obtained from the safety-critical method, which is bounded and practical, and we can see that the nominal control input is only modified in the face of collision threats.

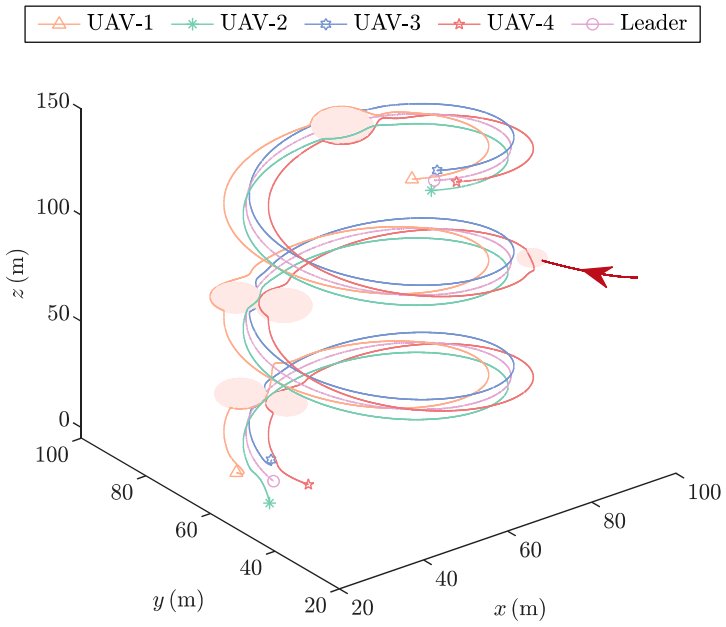


**Figure 2.** The moving trajectories of UAVs.

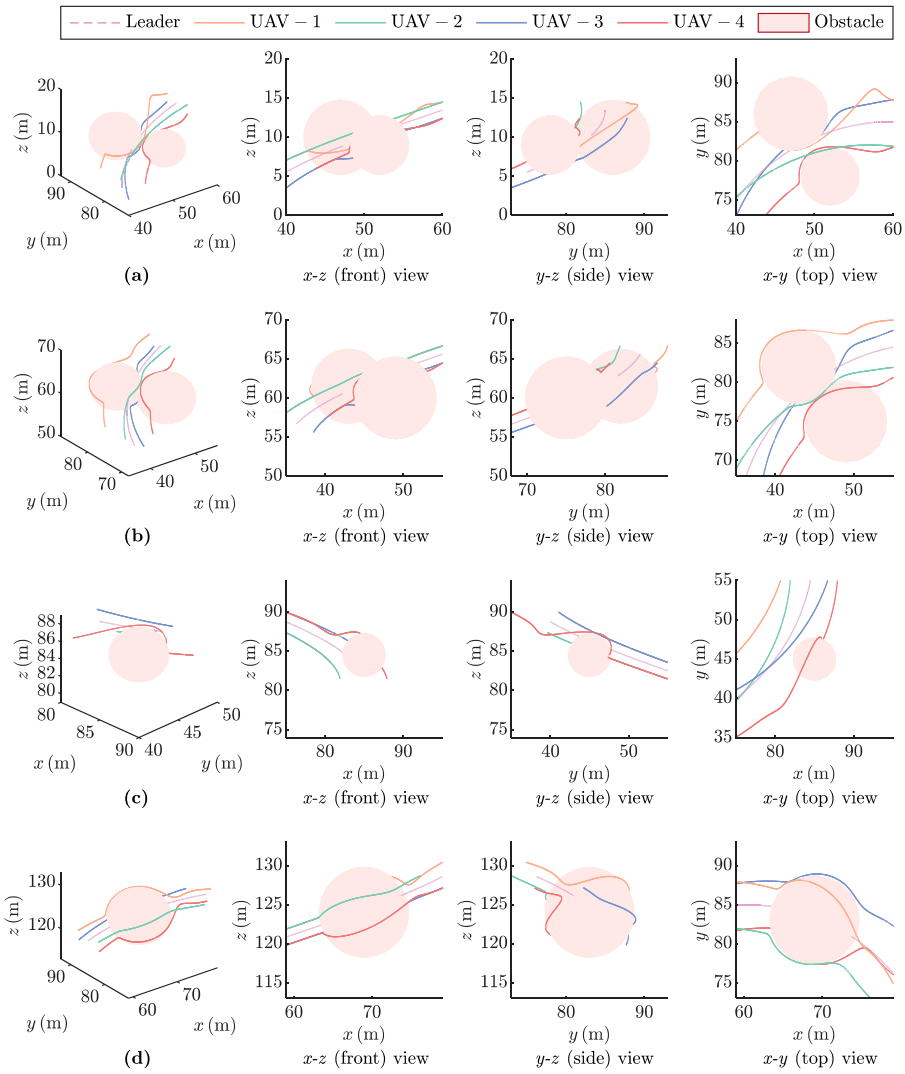


**Figure 3.** Snapshots during obstacle avoidance. (**a**) Obstacles 1 and 2; (**b**) obstacles 3 and 4; (**c**) obstacle 5; (**d**) obstacle 6.

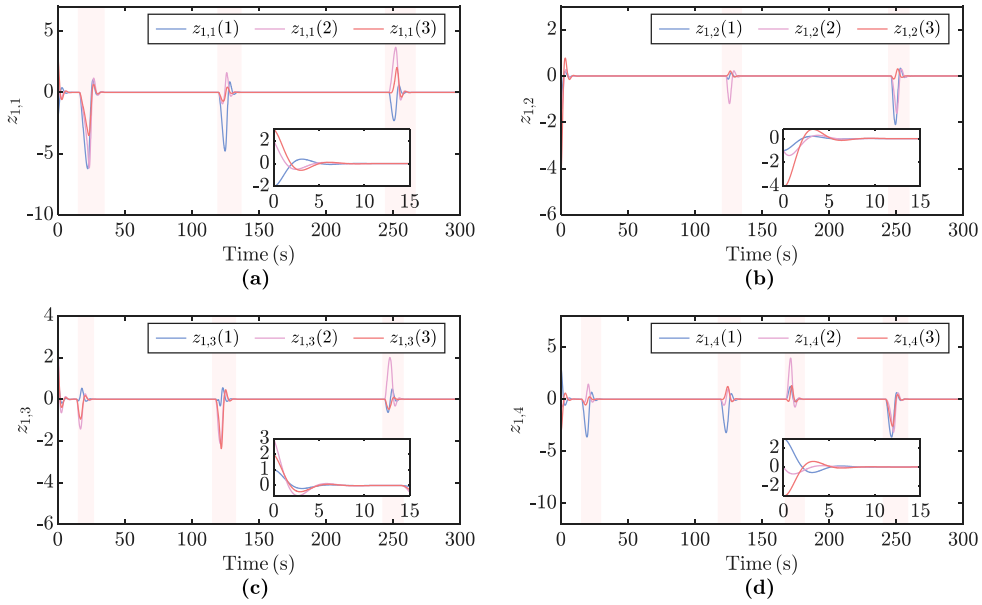


**Figure 4.** The tracking error.

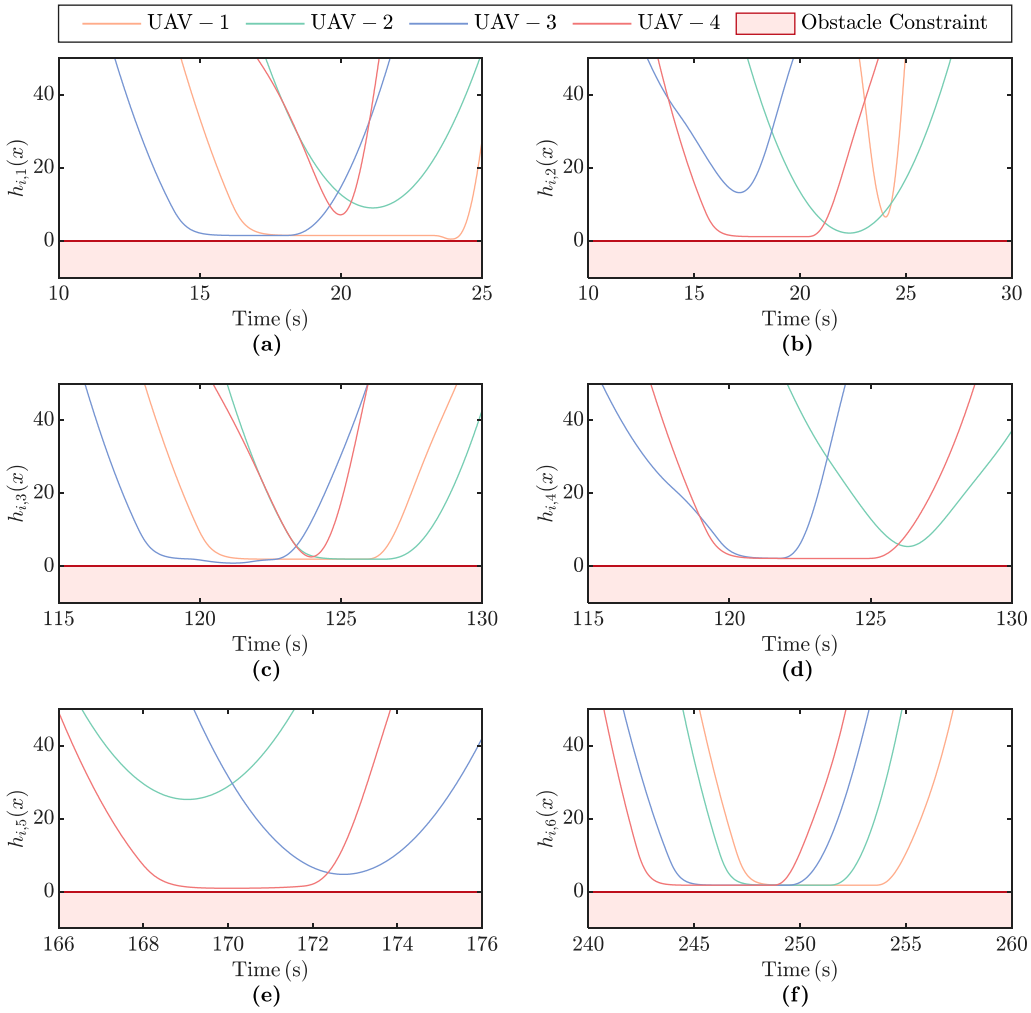


**Figure 5.** The value of $h_{i,j}(\boldsymbol{x})$ with $h_{i,j}(\boldsymbol{x}) = (p_i - p_{ob,j})^T(p_i - p_{ob,j}) - d_{ob,j}^2$, where subscript $i$ denotes the $i$-th UAV and $j$ denotes the $j$-th obstacle.

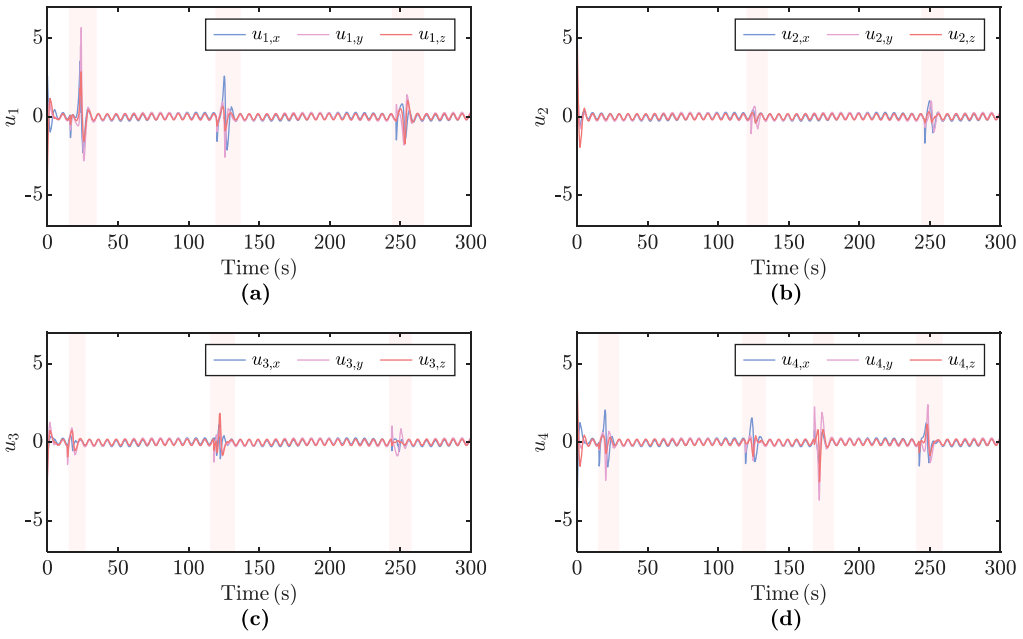


**Figure 6.** The control input.

## 6. Conclusions

In this work, we address the safety-critical fixed-time formation control problem for UAVs with disturbances and obstacle collision threats. First, we design a nominal fixed-time formation control law, in which an elaborate disturbance observer with the sliding mode control strategy is used to estimate the external disturbances. Then, in order to achieve obstacle avoidance and ensure UAVs' safety, we used a CBF-based safety-critical strategy, which can optimize the nominal control law with the constraints constructed using CBFs. Moreover, with some further improvement of the CBF, an exponential CBF is designed so as to provide two relative degree constraints for UAVs. Furthermore, since disturbance may lead to a violation of safety constraints, we design robust safety constraints combining the proposed exponential CBF with min–max inequality, which can ensure UAVs' safety despite disturbances. Simulation experiments demonstrate the validity of the proposed method. In addition, it would be interesting to further reduce the conservativeness of CBFs. Also, the feasibility analysis of CBFs is a meaningful direction for future work.

**Author Contributions:** Conceptualization, Z.S.; methodology, Z.S.; validation, Z.S. and H.H.; writing—original draft preparation, Z.S.; supervision, H.H.; project administration, H.H. All authors have read and agreed to the published version of the manuscript.

**Funding:** This research was funded by the Science Foundation of the Donghai Laboratory, grant number DH-2022ZY0004.

**Institutional Review Board Statement:** Not applicable.

**Informed Consent Statement:** Not applicable.

**Data Availability Statement:** Data is contained within the article.

**Conflicts of Interest:** The authors declare no conflicts of interest.

## References

1. Sarkar, N.I.; Gul, S. Artificial Intelligence-Based Autonomous UAV Networks: A Survey. *Drones* **2023**, *7*, 322. [CrossRef]
2. Muslimov, T.Z.; Munasypov, R.A. Consensus-based cooperative control of parallel fixed-wing UAV formations via adaptive backstepping. *Aerosp. Sci. Technol.* **2021**, *109*, 106416. [CrossRef]
3. Yang, Y.; Xiong, X.; Yan, Y. UAV Formation Trajectory Planning Algorithms: A Review. *Drones* **2023**, *7*, 62. [CrossRef]
4. Han, W.; Wang, J.; Wang, Y.; Xu, B. Multi-UAV Flocking Control with a Hierarchical Collective Behavior Pattern Inspired by Sheep. *IEEE Trans. Aerosp. Electron. Syst.* **2024**, *60*, 2267–2276. [CrossRef]
5. Wu, Y.; Gou, J.; Hu, X.; Huang, Y. A new consensus theory-based method for formation control and obstacle avoidance of UAVs. *Aerosp. Sci. Technol.* **2020**, *107*, 106332. [CrossRef]
6. Tang, J.; Duan, H.; Lao, S. Swarm intelligence algorithms for multiple unmanned aerial vehicles collaboration: A comprehensive review. *Artif. Intell. Rev.* **2023**, *56*, 4295–4327. [CrossRef]
7. Yue, J.; Qin, K.; Shi, M.; Jiang, B.; Li, W.; Shi, L. Event-Trigger-Based Finite-Time Privacy-Preserving Formation Control for Multi-UAV System. *Drones* **2023**, *7*, 235. [CrossRef]
8. Feng, Z.; Hu, G.; Dong, X.; Lu, J. Discrete-time adaptive distributed output observer for time-varying formation tracking of heterogeneous multi-agent systems. *Automatica* **2024**, *160*, 111400. [CrossRef]
9. Wang, B.; Chen, W.; Zhang, B.; Shi, P.; Zhang, H. A Nonlinear Observer-Based Approach to Robust Cooperative Tracking for Heterogeneous Spacecraft Attitude Control and Formation Applications. *IEEE Trans. Autom. Control* **2023**, *68*, 400–407. [CrossRef]
10. Yu, Y.; Chen, J.; Zheng, Z.; Yuan, J. Distributed Finite-Time ESO-Based Consensus Control for Multiple Fixed-Wing UAVs Subjected to External Disturbances. *Drones* **2024**, *8*, 260. [CrossRef]
11. Song, Z.; Wu, Z.; Huang, H. Safety-critical containment control for multi-agent systems with communication delays. *IEEE Trans. Netw. Sci. Eng.* **2024**, *11*, 4911–4922. [CrossRef]
12. Li, L.; Li, Y.; Zhang, Y.; Xu, G.; Zeng, J.; Feng, X. Formation Control of Multiple Autonomous Underwater Vehicles under Communication Delay, Packet Discreteness and Dropout. *J. Mar. Sci. Eng.* **2022**, *10*, 920. [CrossRef]
13. Zhao, W.; Xia, Y.; Zhai, D.-H.; Cui, B. Adaptive event-triggered coordination control of unknown autonomous underwater vehicles under communication link faults. *Automatica* **2023**, *158*, 111277. [CrossRef]
14. Chen, L.; Duan, H. Collision-free formation-containment control for a group of UAVs with unknown disturbances. *Aerosp. Sci. Technol.* **2022**, *126*, 107618. [CrossRef]
15. Li, S.; Wang, X. Finite-time consensus and collision avoidance control algorithms for multiple AUVs. *Automatica* **2013**, *49*, 3359–3367. [CrossRef]

16. Yang, P.; Zhang, A.; Zhou, D. Event-triggered Finite-time Formation Control for Multiple Unmanned Aerial Vehicles with Input Saturation. *Int. J. Control Autom. Syst.* **2021**, *19*, 1760–1773. [CrossRef]
17. Qi, W.-N.; Wu, A.-G.; Huang, J.; Dong, R.-Q. Finite-time attitude consensus control for multiple rigid spacecraft based on distributed observers. *IET Control Theory Appl.* **2023**, *17*, 341–356. [CrossRef]
18. Liu, Y.; Qin, K.; Li, W.; Shi, M.; Lin, B.; Cao, L. Prescribed Performance Rotating Formation Control of Multi-Spacecraft Systems with Uncertainties. *Drones* **2022**, *6*, 348. [CrossRef]
19. Zhang, Y.; Wang, S.-h.; Chang, B.; Wu, W.-h. Adaptive constrained backstepping controller with prescribed performance methodology for carrier-based UAV. *Aerosp. Sci. Technol.* **2019**, *92*, 55–65. [CrossRef]
20. Wu, Q.; Zhu, Q. Prescribed Performance Fault-Tolerant Attitude Tracking Control for UAV with Actuator Faults. *Drones* **2024**, *8*, 204. [CrossRef]
21. Sun, P.; Li, S.; Zhu, B.; Zheng, Z.; Zuo, Z. Vision-based finite-time prescribed performance control for uncooperative UAV target-tracking subject to field of view constraints. *ISA Trans.* **2024**, *149*, 168–177. [CrossRef] [PubMed]
22. Meng, Q.; Ma, Q.; Shi, Y. Adaptive Fixed-Time Stabilization for a Class of Uncertain Nonlinear Systems. *IEEE Trans. Autom. Control* **2023**, *68*, 6929–6936. [CrossRef]
23. Miao, Q.; Zhang, K.; Jiang, B. Fixed-Time Collision-Free Fault-Tolerant Formation Control of Multi-UAVs Under Actuator Faults. *IEEE Trans. Cybern.* **2024**, *54*, 3679–3691. [CrossRef] [PubMed]
24. Yang, Z.; Li, M.; Yu, Z.; Cheng, Y.; Xu, G.; Zhang, Y. Fault Detection and Fault-Tolerant Cooperative Control of Multi-UAVs under Actuator Faults, Sensor Faults, and Wind Disturbances. *Drones* **2023**, *7*, 503. [CrossRef]
25. Jiang, H.; Ma, Q.; Guo, J. Fuzzy-Based Fixed-Time Attitude Control of Quadrotor Unmanned Aerial Vehicle with Full-State Constraints: Theory and Experiments. *IEEE Trans. Fuzzy Syst.* **2024**, *32*, 1108–1115. [CrossRef]
26. Khodaverdian, M.; Hajshirmohamadi, S.; Hakobyan, A.; Ijaz, S. Predictor-based constrained fixed-time sliding mode control of multi-UAV formation flight. *Aerosp. Sci. Technol.* **2024**, *148*, 109113. [CrossRef]
27. Jia, J.; Chen, X.; Wang, W.; Liao, H.; Xie, M. Collision avoidance in target encirclement and tracking of unmanned aerial vehicles under a dynamic event-triggered formation control. *Control Eng. Pract.* **2024**, *142*, 105781. [CrossRef]
28. Cui, G.; Xu, H.; Chen, X.; Yu, J. Fixed-Time Distributed Adaptive Formation Control for Multiple QUAVs with Full-State Constraints. *IEEE Trans. Aerosp. Electron. Syst.* **2023**, *59*, 4192–4206. [CrossRef]
29. Zheng, R.; Zhu, Q.; Huang, S.; Du, Z.; Shi, J.; Lyu, Y. Extended State Observer-Based Sliding-Mode Control for Aircraft in Tight Formation Considering Wake Vortices and Uncertainty. *Drones* **2024**, *8*, 165. [CrossRef]
30. Lei, Y.; Fu, R. Disturbance-Observer-based Fast Terminal Sliding Mode Control for Quadrotor UAVs. In Proceedings of the Chinese Control and Decision Conference (CCDC), Yichang, China, 20–22 May 2023; pp. 953–958.
31. Ma, Z.; Gong, H.; Wang, X. Fault-Tolerant Event-Triggrred Control for Multiple UAVs with Predefined Tracking Performance. *Drones* **2024**, *8*, 25. [CrossRef]
32. Cao, L.; Li, H.; Wang, N.; Zhou, Q. Observer-Based Event-Triggered Adaptive Decentralized Fuzzy Control for Nonlinear Large-Scale Systems. *IEEE Trans. Fuzzy Syst.* **2019**, *27*, 1201–1214. [CrossRef]
33. Song, Z.; Xie, M.; Huang, H. Bearing-Only Formation Tracking Control for Multi-Agent Systems with Time-Varying Velocity Leaders. *IEEE Control Syst. Lett.* **2024**, *8*, 2027–2032. [CrossRef]
34. Wang, J.; Bi, C.; Wang, D.; Kuang, Q.; Wang, C. Finite-time distributed event-triggered formation control for quadrotor UAVs with experimentation. *ISA Trans.* **2022**, *126*, 585–596. [CrossRef] [PubMed]
35. Zhou, Z.; Wang, H.; Hu, Z.; Wang, Y.; Wang, H. A Multi-Time-Scale Finite Time Controller for the Quadrotor UAVs with Uncertainties. *J. Intell. Robot. Syst.* **2019**, *94*, 521–533. [CrossRef]
36. Sun, L.; Sun, G.; Jiang, J. Disturbance observer-based saturated fixed-time pose tracking for feature points of two rigid bodies. *Automatica* **2022**, *144*, 110475. [CrossRef]
37. Rezaei, E.; Bolandi, H.; Fathi, M. Designing a fixed-time observer-based adaptive non-singular sliding mode controller for flexible spacecraft. *ISA Trans.* **2024**, *148*, 32–44. [CrossRef]
38. Sui, B.; Zhang, J.; Liu, Z.; Wei, J. Fixed-Time Trajectory Tracking Control of Fully Actuated Unmanned Surface Vessels with Error Constraints. *J. Mar. Sci. Eng.* **2024**, *12*, 584. [CrossRef]
39. Zhang, P.; He, Y.; Wang, Z.; Li, S.; Liang, Q. Research on Multi-UAV Obstacle Avoidance with Optimal Consensus Control and Improved APF. *Drones* **2024**, *8*, 248. [CrossRef]
40. Liu, Y.; Chen, C.; Wang, Y.; Zhang, T.; Gong, Y. A fast formation obstacle avoidance algorithm for clustered UAVs based on artificial potential field. *Aerosp. Sci. Technol.* **2024**, *147*, 108974. [CrossRef]
41. Qian, M.; Wu, Z.; Jiang, B. Cerebellar Model Articulation Neural Network-Based Distributed Fault Tolerant Tracking Control with Obstacle Avoidance for Fixed-Wing UAVs. *IEEE Trans. Aerosp. Electron. Syst.* **2023**, *59*, 6841–6852. [CrossRef]
42. Singletary, A.; Klingebiel, K.; Bourne, J.; Browning, A.; Tokumaru, P.; Ames, A. Comparative Analysis of Control Barrier Functions and Artificial Potential Fields for Obstacle Avoidance. In Proceedings of the IEEE/RSJ International Conference on Intelligent Robots and Systems (IROS), Prague, Czech Republic, 27 September–01 October 2021; pp. 8129–8136.
43. Ames, A.D.; Xu, X.; Grizzle, J.W.; Tabuada, P. Control Barrier Function Based Quadratic Programs for Safety Critical Systems. *IEEE Trans. Autom. Control* **2017**, *62*, 3861–3876. [CrossRef]
44. Li, B.; Wen, S.; Yan, Z.; Wen, G.; Huang, T. A Survey on the Control Lyapunov Function and Control Barrier Function for Nonlinear-Affine Control Systems. *IEEE/CAA J. Automat. Sin.* **2023**, *10*, 584–602. [CrossRef]

45. Hegde, A.; Ghose, D. Collaborative Guidance of UAV-Transported Semi-Flexible Payloads in Environments with Obstacles. In Proceedings of the IEEE Conference on Decision and Control (CDC), Austin, TX, USA, 13–17 December 2021; pp. 490–495.
46. Lin, J.; Miao, Z.; Wang, Y.; Wang, H.; Wang, X.; Fierro, R. Vision-Based Safety-Critical Landing Control of Quadrotors with External Uncertainties and Collision Avoidance. *IEEE Trans. Control. Syst. Technol.* **2024**, *32*, 1310–1322. [CrossRef]
47. Wu, G.; Sreenath, K. Safety-Critical Control of a Planar Quadrotor. In Proceedings of the American Control Conference (ACC), Boston, MA, USA, 6–8 July 2016; pp. 2252–2258.
48. Xiao, W.; Belta, C. Control Barrier Functions for Systems with High Relative Degree. In Proceedings of the IEEE Conference on Decision and Control (CDC), Nice, France, 11–13 December 2019; pp. 474–479.
49. Kim, S.-J.; Suh, J.-H. Model-Free RBF Neural Network Intelligent-PID Control Applying Adaptive Robust Term for Quadrotor System. *Drones* **2024**, *8*, 179. [CrossRef]
50. Jagtap, P.; Pappas, G.J.; Zamani, M. Control Barrier Functions for Unknown Nonlinear Systems using Gaussian Processes. In Proceedings of the IEEE Conference on Decision and Control (CDC), 14–18 December 2020; pp. 3699–3704.
51. Zhao, P.; Mao, Y.; Tao, C.; Hovakimyan, N.; Wang, X. Adaptive Robust Quadratic Programs using Control Lyapunov and Barrier Functions. In Proceedings of the IEEE Conference on Decision and Control (CDC), 14–18 December 2020; pp. 3353–3358.
52. Rasmussen, C.E.; Williams, C.K.I. *Gaussian Processes for Machine Learning*; MIT Press: Cambridge, MA, USA, 2006; Volume 2.
53. Kolathaya, S.; Ames, A.D. Input-to-State Safety with Control Barrier Functions. *IEEE Control Syst. Lett.* **2019**, *3*, 108–113. [CrossRef]
54. Alan, A.; Taylor, A.J.; He, C.R.R.; Ames, A.D.; Orosz, G. Control Barrier Functions and Input-to-State Safety with Application to Automated Vehicles. *IEEE Trans. Control Syst. Technol.* **2023**, *31*, 2744–2759. [CrossRef]
55. Buch, J.; Liao, S.-C.; Seiler, P. Robust Control Barrier Functions with Sector-Bounded Uncertainties. *IEEE Control Syst. Lett.* **2022**, *6*, 1994–1999. [CrossRef]
56. Shao, S.; Xu, S.; Zhao, Y.; Wu, X. Unknown Input Observer-Based Fixed-Time Trajectory Tracking Control for QUAV with Actuator Saturation and Faults. *Drones* **2023**, *7*, 344. [CrossRef]
57. Xie, T.; Xian, B.; Gu, X.; Hu, J.; Liu, M. Disturbance Observer-Based Fixed-Time Tracking Control for a Tilt Trirotor Unmanned Aerial Vehicle. *IEEE Trans. Ind. Electron.* **2024**, *71*, 3894–3903. [CrossRef]
58. Ai, X.; Yu, J. Fixed-time trajectory tracking for a quadrotor with external disturbances: A flatness-based sliding mode control approach. *Aerosp. Sci. Technol.* **2019**, *89*, 58–76. [CrossRef]
59. Gao, S.; Peng, Z.; Wang, H.; Liu, L.; Wang, D. Safety-Critical Model-Free Control for Multi-Target Tracking of USVs with Collision Avoidance. *IEEE/CAA J. Automat. Sin.* **2022**, *9*, 1323–1326. [CrossRef]
60. Du, H.; Zhu, W.; Wen, G.; Wu, D. Finite-time formation control for a group of quadrotor aircraft. *Aerosp. Sci. Technol.* **2017**, *69*, 609–616. [CrossRef]
61. Polyakov, A. Nonlinear Feedback Design for Fixed-Time Stabilization of Linear Control Systems. *IEEE Trans. Autom. Control* **2012**, *57*, 2106–2110. [CrossRef]
62. Hardy, G.H.; Littlewood, J.E. *; Pólya., G. Inequalities*; Cambridge University Press: Cambridge, UK, 1952.
63. Liu, Z.; Liu, J.; Zhang, O.; Zhao, Y.; Chen, W.; Gao, Y. Adaptive Disturbance Observer-Based Fixed-Time Tracking Control for Uncertain Robotic Systems. *IEEE Trans. Ind. Electron.* **2024**, *71*, 14823–14831. [CrossRef]
64. Ames, A.D.; Coogan, S.; Egerstedt, M.; Notomista, G.; Sreenath, K.; Tabuada, P. Control Barrier Functions: Theory and Applications. In Proceedings of the European Control Conference (ECC), Naples, Italy, 25–28 June 2019; pp. 3420–3431.
65. Wang, H.; Shan, J. Fully Distributed Event-Triggered Formation Control for Multiple Quadrotors. *IEEE Trans. Ind. Electron.* **2023**, *70*, 12566–12575. [CrossRef]